Rev. Roum. Sci. Techn.– Électrotechn. et Énerg.
Vol. **70**, *1*, pp. 27–32, Bucarest, 2025

COMPLEMENTS REGARDING THE DYNAMIC STABILITY OF THE SYNCHRONOUS MACHINE

AUREL CAMPEANU[1], IOAN CAUTIL[1], ALEXANDRU CALINA[1], ION VLAD[1], MONICA-ADELA ENACHE[1]

Keywords: Dynamic stability; Synchronous machine; Mathematical dynamic models.

This paper analyzes factors conditioning the dynamic stability of a high-power synchronous motor, by using non-linear dynamic mathematical models. There is noticed a structural difference between the dynamic angular characteristics compared to the static angular characteristics. There results in notable electrical, magnetic and mechanical stresses, which must be necessarily considered, in the stage of design and exploitation.

1. INTRODUCTION

Substantiations of the dynamic processes of alternating current electrical machines emerge as an objective today, when they, bounded to automatic systems of starting, braking, reversals, in well-defined time durations, operates in some conditions which are far from the steady state ones, well known.

The main purpose of the present research is to establish some dynamic mathematical models, so that simulations catch the fundamental processes in a such extent which enables a quantitative evaluation, within acceptable practical limits, of the electromagnetic, mechanical and thermal stresses, specific to strongly unsteady regimes [1–14]. The original contributions are presented in [15–1]. Specific simulations become compulsory in the dedicated design and in the efficient steady-state and dynamic exploitation of electrical machines, in accordance with the nowadays exigencies [22–29]. An exhaustive analysis of the dynamic processes is approached in [20].

This paper expresses the dynamic stability of a high-power synchronous motor, subjected to different shocks of load. The parameters of the motor are mentioned in the Appendix.

2. THE MATHEMATICAL MODEL

The mathematical model is written in the two-axes theory, and regards a solution together of the voltage equations which catch the electrical inertia as in [15,17,25], *etc*.

$$[u] = A\frac{\mathrm{d}X}{\mathrm{d}t} + BX;\ \ [u] = \begin{bmatrix} u_d & u_q & u_E & 0 & 0 \end{bmatrix}^T, \tag{1}$$

and the motion equation which considers mechanical inertia,

$$m - M_r = \frac{J}{p}\frac{\mathrm{d}\omega}{\mathrm{d}t} \tag{2}$$

For the currents i_s, i_E, i_D, i_Q, as state variables

$$X = \begin{bmatrix} i_d & i_q & i_E & i_D & i_Q \end{bmatrix}^T \tag{3}$$

The corresponding matrices are

$$A = \begin{bmatrix} L_{s\sigma} + L_{mdt} & 0 & L_{mdt} & L_{mdt} & 0 \\ 0 & L_{s\sigma} + L_{mq} & 0 & 0 & L_{mq} \\ L_{mdt} & 0 & L_{E\sigma} + L_{mdt} & L_{mdt} & 0 \\ L_{mdt} & 0 & L_{mdt} & L_{D\sigma} + L_{mdt} & 0 \\ 0 & L_{mq} & 0 & 0 & L_{Q\sigma} + L_{mq} \end{bmatrix} \tag{4}$$

$$B = \begin{bmatrix} R_s & -\omega\left(L_{s\sigma} + L_{mq}\right) & 0 & 0 & -\omega L_{mq} \\ \omega\left(L_{s\sigma} + L_m d\right) & R_s & \omega L_{md} & \omega L_{md} & 0 \\ 0 & 0 & R_E & 0 & 0 \\ 0 & 0 & 0 & R_D & 0 \\ 0 & 0 & 0 & 0 & R_Q \end{bmatrix} \tag{5}$$

The electromagnetic torque is

$$m = \frac{3}{2}p\left[\left(L_{md} - L_{mq}\right)i_d i_q + L_{md}\left(i_D + i_E\right)i_q - L_{mq} i_d i_Q\right]. \tag{6}$$

The model considers the magnetic asymmetry and the magnetic saturation, static and dynamic one, along the *d*-axis. The notations used are widely accepted in literature.

3. SIMULATIONS RESULTS

There have been plotted the dynamic electromagnetic torques in (m,t), (m,ω), (m,θ) coordinates, the internal angle θ, the currents i_s, i_E, i_D, i_Q of the windings, the magnetization inductances, static and dynamic ones, L_{md}, L_{mdt} and the correlated evolution of the electrical angular speed and of the main rotating field ω_ψ and the rotor one, ω. There have been emphasized the variations versus time defined by the zones **a** (starting period – t = (0-7) s), **b** (applying the excitation t = (7-23) s), **c** (loading by jump at resistant torque M_r – t > 23 s), **d** (considering other excitation currents). The points **1, 2, 3** signify the end, by synchronization, of the zones **a, b, c**.

CONSIDER M_R = 40000 NM, U_E = 2,1 V.

For an overall assessment, in certain graphs, all the zones **a, b, c** was considered. Fig.1 provides valuable qualitative and quantitative information regarding electromagnetic torque. There result important values anticipated in the zone **a** and insignificant variations in the zone **b**; in the zone **c**, of interest, some fast oscillations occur, having a short duration, specific to an subtransient dynamic process, considerably reduced in comparison with the ones from the zone **a**, but important relatively to M_r. Fig. 2 emphasizes the final part of the oscillations evoked in the zone **c** and the duration for obtaining the steady-state operation from the point **3** owed to the significant time constant of the excitation winding, E.

The static and dynamic angular characteristics (corresponding to the oscillations from the zone c in Fig.1), structurally different, are plotted together in Fig. 3 [20].
The precise positioning in point **3** on the static characteristic validates in a convincing manner their establishing. Fig. 4 presents the characteristic $\theta(t)$. The zone **b** is in accordance with the graph $i_E(t)$ plotted in Fig. 6.

The currents $i_s(t)$, $i_E(t)$, $i_D(t)$, $i_Q(t)$ are plotted in Fig. 5 – Fig. 8. Important values of all the currents of the machine

[1] Faculty of Electrical Engineering, University of Craiova, 107 Decebal Street, Craiova, Romania.
E-mails: acampeanu@em.ucv.ro, ivlad@em.ucv.ro, menache@em.ucv.ro

DOI: 10.59277/RRST-EE.2025.1.5

windings occur in zone **a**, and in the zone of applying the torque M_r.

The short-term sign changing of $i_E(t)$ in the zone **b**, is caused by the polar-pitch rotation of the rotor when applying $u_E = 2{,}1$ V.

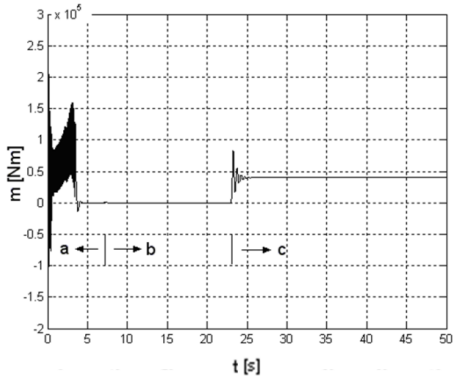

Fig. 1 – Characterfistic m(t).

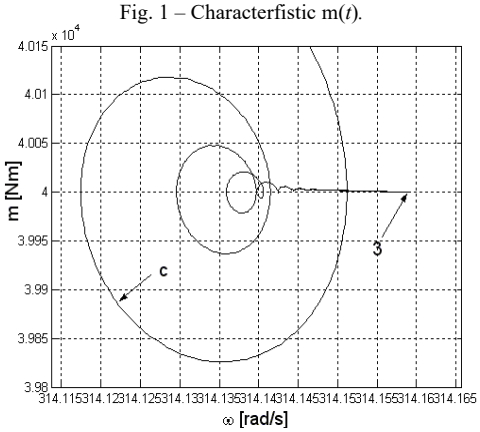

Fig. 2 – Characteristic m(θ) – detail at the final part of the zone **c**.

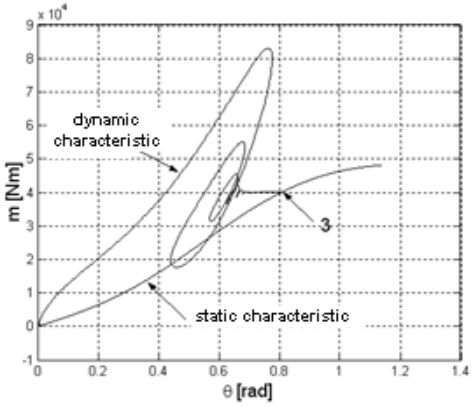

Fig. 3 – Characteristics m(θ), static and dynamic.

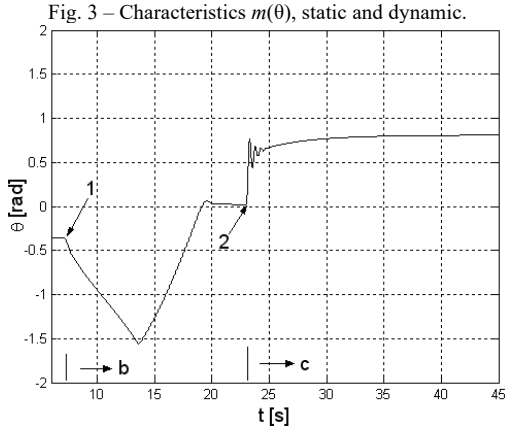

Fig. 4 – Characteristic θ(t) – detail in zones **b, c**.

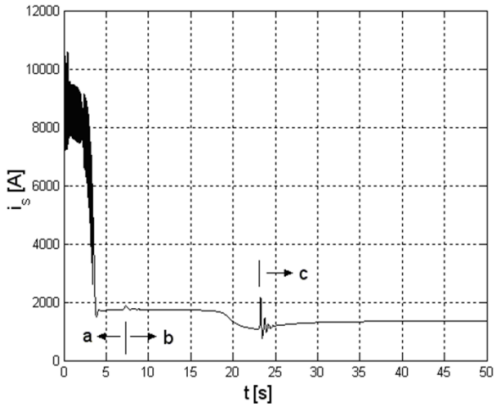

Fig. 5 – Characteristic $i_S(t)$.

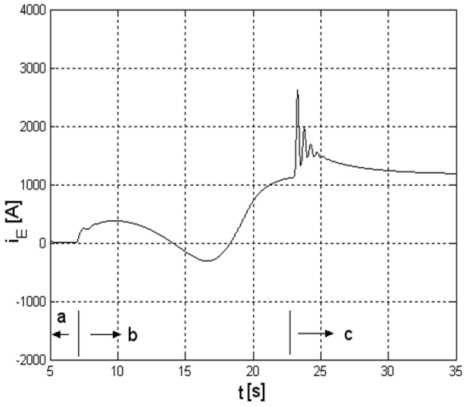

Fig. 6 – Characteristic $i_E(t)$ – detail in zones **b, c**.

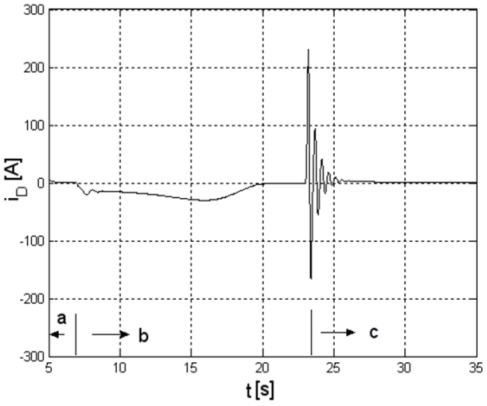

Fig. 7 – Characteristic $i_D(t)$ – detail in zones **b, c**.

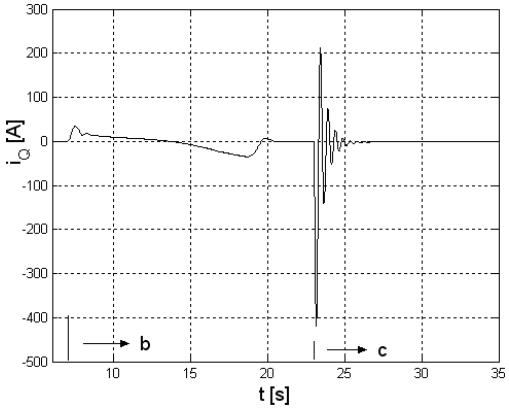

Fig. 8 – Characteristic $i_Q(t)$ – detail in zones **b, c**.

The evolutions of the currents $i_D(t)$, $i_Q(t)$ have the same justifications as above. In the final part of the zones **a** and **c,**

they cancel.

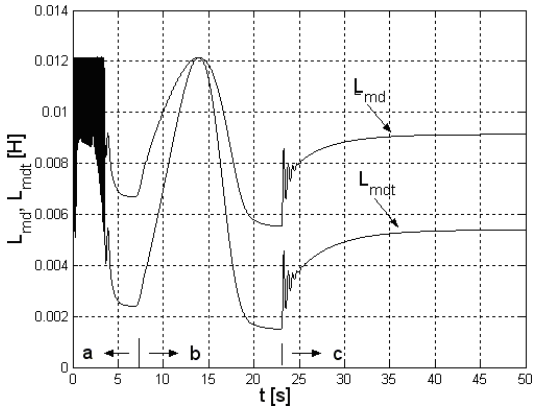

Fig. 9 – Characteristics $L_{md}(t)$, $L_{mdt}(t)$.

The variations of the magnetic stresses, in accordance with the ones presented above, are plotted in Fig. 9 in all the zones and emphasize the importance of considering magnetic saturation in mathematical models.

CONSIDER M_R = 50000 NM.

The characteristic $m(t)$ in the zone **c** is plotted in Fig. 10 [20]**.** Applying M_r causes the same subtransient oscillations, obviously having larger amplitudes, followed by an apparent synchronous stabilization; at $t > 70$ s a permanent asynchronous operation occurs, with fast oscillations, significantly larger, complicated by the magnetic asymmetry, separated by some intermediary zones of synchronism.

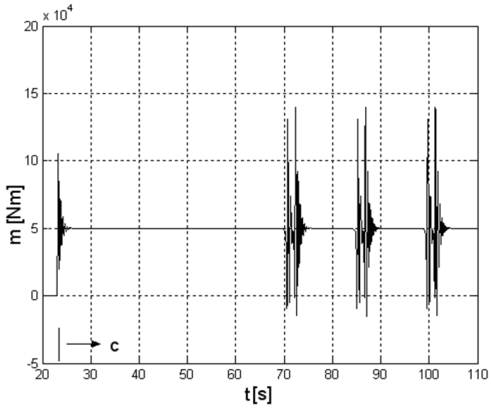

Fig. 10 – Characteristic $m(t)$ in the zone **c**.

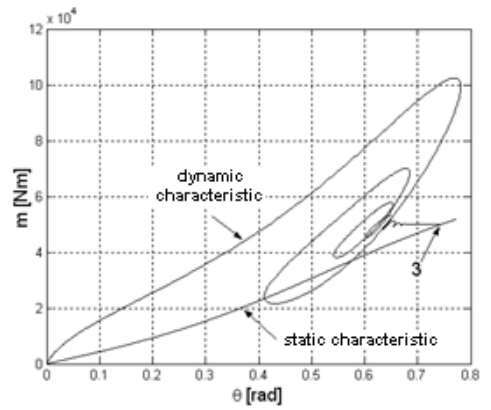

Fig. 11 – Characteristics $m(\theta)$, static and dynamic.

Plotting together the static and dynamic characteristics in Fig.11, introducing u_E = 3 V previously to the shock M_r avoids the asynchronous evolution and restore synchronism in point **3**.

The qualitative aspect of the dynamic characteristic is like the one depicted in Fig. 3.

The currents $i_S(t)$ and $i_E(t)$ (Fig. 12, respectively Fig. 13) provide quantitative information regarding very large amplitudes in the oscillating zone c.

Analogously, the current $i_D(t)$, $i_Q(t)$ are found.

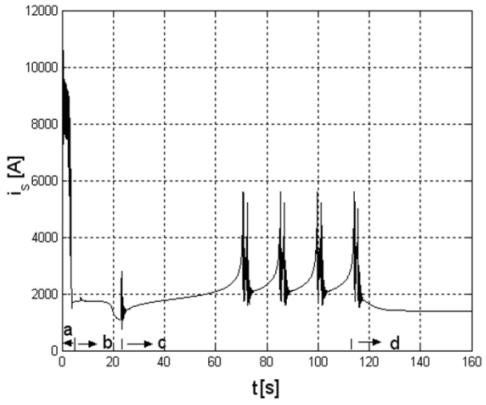

Fig. 12 – Characteristic $i_S(t)$.

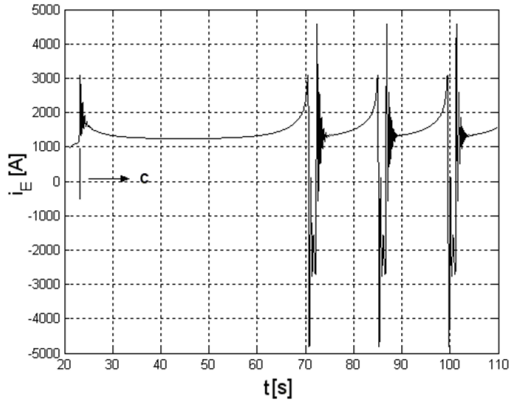

Fig. 13 – Characteristic $i_E(t)$ in the zone **c**.

To avoid the oscillating asynchronous operation, the voltage u_E = 3 V is applied at t = 50 s. The dynamic evolutions and the synchronous operation follow a practically electromagnetic transient process, very favorable. The characteristics $m(t)$, $\theta(t)$, $i_S(t)$, $i_E(t)$, $L_{md}(t)$, $L_{mdt}(t)$ are plotted in Fig. 14 – Fig. 18.

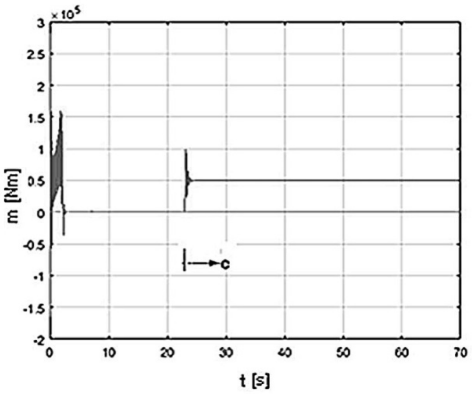

Fig. 14 – Characteristic $m(t)$ in the zones **a - d**.

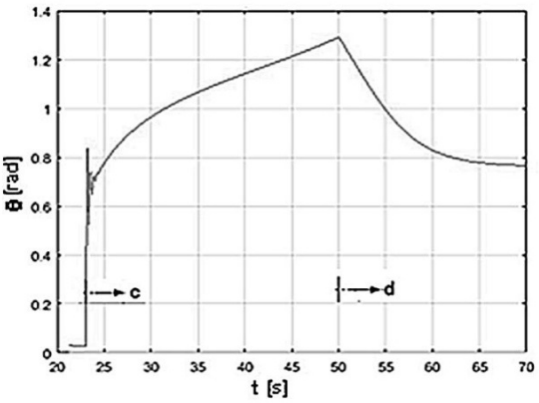

Fig. 15 – Characteristic θ(*t*) – detail in the zones **c, d**.

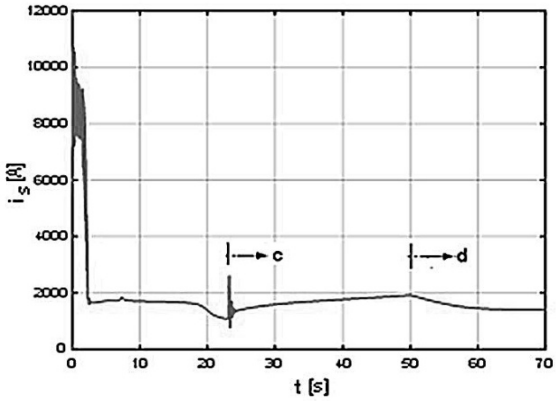

Fig. 16 – Characteristic $i_s(t)$ in the zones **a - d**.

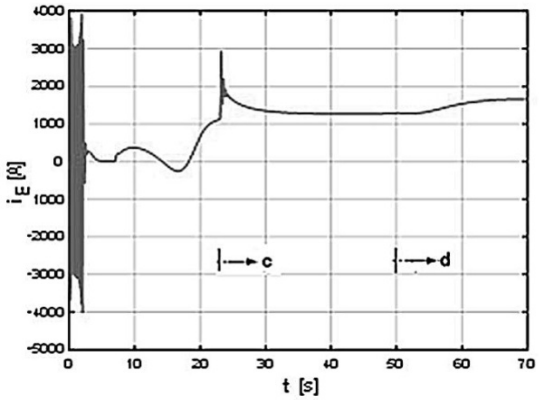

Fig. 17 – Characteristic $i_E(t)$ in the zones **a - d**.

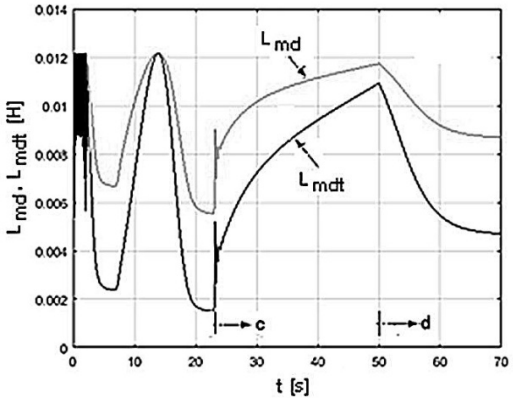

Fig. 18 – Characteristics $L_{md}(t)$, $L_{mdt}(t)$ in the zones **a - d**.

Consider M_r = 60000 Nm.

In case u_E = 2.1 V a strongly asynchronous operation results in the zone **c**, which increases by increasing the excitation to u_E = 4 V at t = 50 s (zone **d**).

In Fig.19 there is depicted the dynamic electromagnetic torque, *m(t)* in all zones.

Considering u_E = 4 V, as well as the graphs from Fig. 11 avoid the asynchronous operation; point **3** is found on both angular characteristics.

In [20] a detailed analysis of the electromagnetic torque in the (m, ω), (m, θ) coordinates.

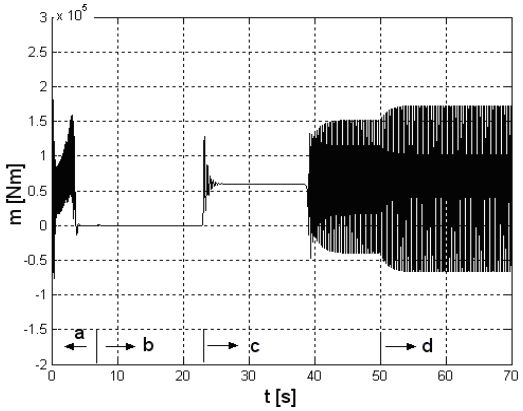

Fig. 19 – Characteristic *m(t)*.

The currents $i_s(t)$ and $i_E(t)$ in conditions u_E = 4 V are plotted in Fig. 20, respectively in Fig. 21.

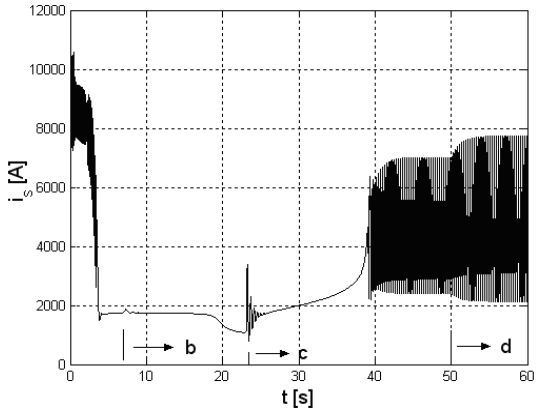

Fig. 20 – Characteristics $i_s(t)$.

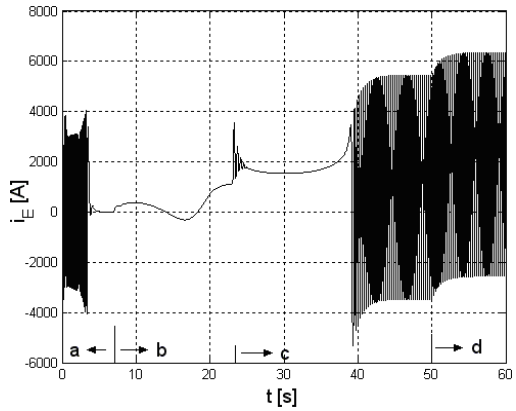

Fig. 21 – Characteristic $i_E(t)$.

Applying the voltage u_E = 4 V in zone **c,** previously to occurring the asynchronous operation (t = 36 s) removes, as in case M_r = 50000 Nm the high-oscillating electromagnetic and mechanical stresses.

There are obtained the representative characteristics from Fig. 22 – Fig. 26, ensuring, slowly and without practical shocks, the synchronism, specific to an electromagnetic transient regime.

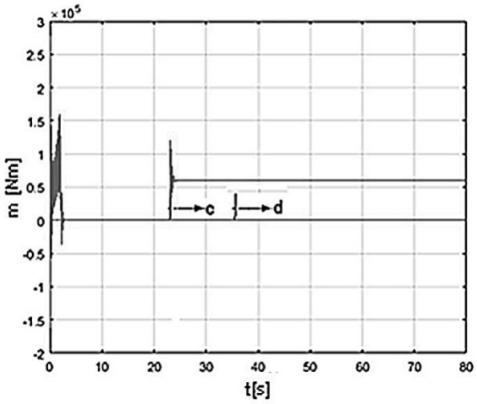

Fig. 22 – Characteristic $m(t)$ in the zones **a - d**.

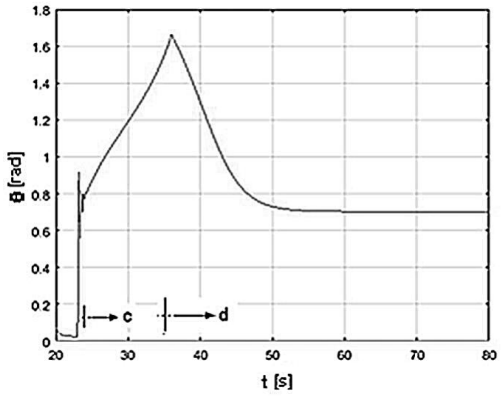

Fig. 23 – Characteristic $\theta(t)$ – detail in the zones **c, d**.

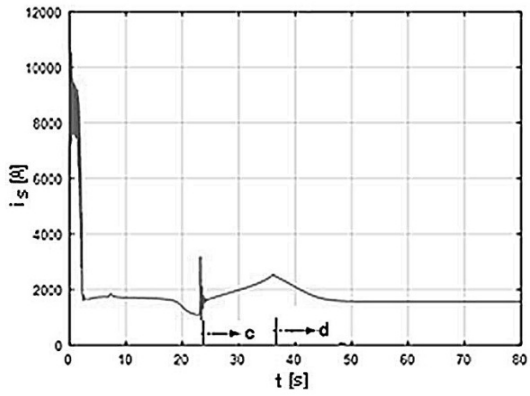

Fig. 24 – Characteristic $i_s(t)$ in the zones **a - d**.

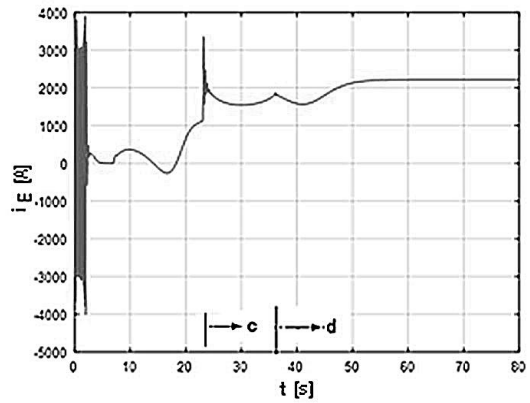

Fig. 25 – Characteristic $i_E(t)$ in the zones **a - d**.

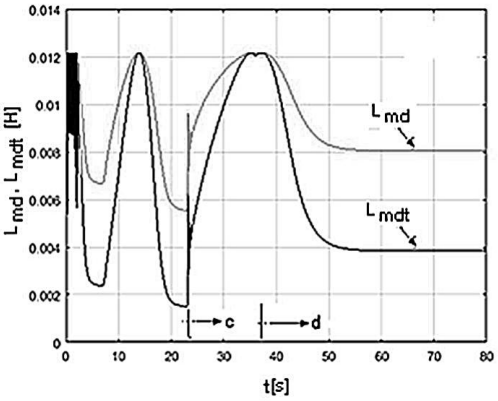

Fig. 26 – Characteristics $L_{md}(t)$, $L_{mdt}(t)$ in the zones **a - d**.

4. CONCLUSIONS

In analyzing dynamic stability, using dynamic mathematical models is compulsory to establish the real dimensions of the electromagnetic and mechanical stresses.

In the first moments of applying M_r, the subtransient components of the machine currents occur for a short period of time, consequently, significant oscillating values of the electromagnetic torques also happen.

The speeds ω, ω_ψ oscillate, too, tightly correlated around ω_1. The subtransient zone is essentially dependent on M_r.

At the end of the subtransient zone the currents of the damping windings vanish. An apparent synchronous operation is established in which $m(t) = M_r$, and $\omega(t) = \omega_\psi(t) = \omega_1$ (Fig.1 – Fig.9). The steady synchronous operation results at the damping of the transient currents i_s, i_E, practically with the critical time constant of the excitation winding.

At an increased M_r (Fig. 10– Fig.2 6), the apparent synchronous operation might degenerate in an asynchronous oscillating one, characterized by currents of all the machine windings and electromagnetic torques, having sensitively higher values than the ones corresponding to the subtransient zone.

If u_E increases within this time interval, including the asynchronous one, it is possible to recover synchronism, without load shocks (the dynamic process practically becomes, as above, an electromagnetic one).

Synchronism only becomes possible if the speed oscillations of the rotor are around the synchronism speed ω_1. If this condition is not fulfilled, an increase of u_E worsens the oscillating asynchronous operation.

Static and dynamic electromagnetic stresses vary within significant limits and must be considered for precision determination. Irrespective of how the coordinates of point **3** are reached, they are found on the static angular characteristics. The steady-state and dynamic mathematical models used are confirmed on this basis.

The values of M_r have been chosen to emphasize the main specific aspects of dynamic stability.

Forcing the excitation simultaneously with applying M_r is not compulsory; the available time interval in case of high-power machines is of the order of seconds or tens of seconds and reduces as M_r increases.

APPENDIX

P_n = 8000 kW, U_n = 2887/5000 V, n_1 = 1500 rpm, f = 50 Hz, $R_s = 32.967 \cdot 10^{-3}$ Ω, $L_{s\sigma} = 0.795 \cdot 10^{-3}$H, $L_{E\sigma} = 1.823 \cdot 10^{-3}$H, $L_{D\sigma} = 0.838 \cdot 10^{-3}$H, $L_{Q\sigma} = 0.921 \cdot 10^{-3}$H, $L_{mq} = 6.98 \cdot 10^{-3}$H, $R_E = 1.798 \cdot 10^{-3}$Ω, $R_D = 92.046 \cdot 10^{-3}$Ω, $R_Q = 115.05 \cdot 10^{-3}$Ω, J = 616 kg m^2.

The saturation characteristic is

$$\psi_m(i_{md}) = 1.09 \times 9.189 \text{atan} \frac{i_{md}}{823.867}.$$

ACKNOWLEDGMENT

Source of research funding in this article: Research program of the Electrical Engineering Faculty Craiova (financed by the University of Craiova).

CREDIT AUTHORSHIP CONTRIBUTION

Author_1: 50%
Author_2: 20%
Author_3: 10%
Author_4: 10%
Author_5: 10%.

Received on 12 December 2024

REFERENCES

1. B. Adkins, *The General Theory of Electrical Machines*, J. Wiley, New York (1959).
2. I. Boldea, *Electric Machine Parameters* (in Romanian), Ed. Academiei (1991).
3. N. Canay, *Allgemeine theorie der sinchn-und asynchronmachines in der operator –matrix –darstellung*, Archiv fur Elektrotechnik, **46**, *2*, pp.83–102 (1961).
4. C.H. Concordia, *Synchronous Machines*, J. Willey, New York (1951).
5. I. Dumitrache, *Automatica*, Ed. Academiei Romane, Bucuresti (2016).
6. E.I. Kazovschi, *Perehodnîe Procesî Electriceschih Maşinah per. Toka*, Ecad. Sc., Moscow–Leningrad (1962).
7. P. Krause, *Analysis of Electric Machinery*, Mc Graw-Hill, New York (1986).
8. K.P. Kovacs, I. Racz, *Transient Regimes of A.C. Machines*, Springer Verlag (1995).
9. T.H. Laible, *Die Theorie der Synchonmaschine in nichtstationaren Betrieb*, Springer Verlag, Berlin (1952).
10. E. Levi, *Saturation modeling in D-Q axis models of salient pole synchronous machines*, IEEE Trans. On Energy Conversion, **14**, *1*, pp. 44–50 (1999).
11. V. Lyon, *Transient Analysis of A.C. Machinery*, J. Wiley, New York (1954).
12. P. Vas, *Generalized analysis of saturated AC machines*, Archiv f. Elektrotechnik, **64**, *1–2* (1981).
13. J.H. Walker, *Large Synchronous Machines: Design, Manufacture and Operation*, Oxford, UK, Clarendon (1981).
14. I. Boldea, *Variable Speed Generators*, CRC Press, Boca Raton, FL (2016).
15. A. Câmpeanu, *About the saturation effect in the alternative current machine equations*, Rev. Roum. Sci. Techn. – Électrotechn. et Énerg, **38**, *4*, pp. 539–546 (1993).
(16) A. Câmpeanu, *Transient performance of the saturated induction machine*, Electrical Engineering, Archiv fur Elektrotechnik, **78**, *4*, pp. 241–247 (1995).
(17) A. Câmpeanu, *Nonlinear dynamical models of saturated salient pole synchronous machine*, Rev. Roum. Sci. Techn. – Électrotechn. et Énerg., **47**, *3*, pp. 307–317 (2002).
(18) A. Câmpeanu, S. Ivanov, *Recurrence relations in saturated AC machines modeling*, EPE – PMC, Riga (2004).
(19) A. Câmpeanu, *Maşini electrice. Probleme fundamentale, speciale şi de funcţionare optimala*, Editura Scrisul Românesc (1987).
(20) A. Câmpeanu, R. Munteanu, I.V. Iancu, *About dynamic stability of high-power synchronous machine. A review*, Rev. Roum. Sci. Techn. – Électrotechn. et Énerg., **62**, *1*, Bucharest (2017).
(21) A. Câmpeanu, *Über eine besondere betriebsweise von synchronmaschinen*, Archiv fur Elektrotechnik, **61**, pp. 33–40 (1979).
(22) A. Câmpeanu, I. Cauti, *On the transient behavior of saturated synchronous machines*, Rev. Roum. Sci. Techn. – Électrotechn. et Énerg., **53**, *4*, pp. 367–376 (2008).
(23) A. Câmpeanu, M. Stiebler, *Modeling of saturation in salient pole synchronous machine*, Proc. of OPTIM, Braşov, Romania (2010).
(24) A. Câmpeanu, M. Stiebler, *Modeling and simulation of dynamical processes in high power salient pole synchronous machines*, Rev. Roum. Sci. Techn. – Électrotechn. et Énerg., **56**, *2*, pp. 179–188 (2011).
(25) A. Câmpeanu, S. Enache, I. Vlad, G. Liuba, L. Augustinov, I. Cauti, *Simulation of asynchronous operation in high power salient pole synchronous machines*, Proc. ICEM, Marseille (2012).
(26) A. Câmpeanu, I. Vlad, T. Cimpeanu, S. Enache, I. Cauti, *Simulation of dynamic single supply back-to-back high-power synchronous machines operation*, Rev. Roum. Sci. Techn. – Électrotechn. et Énerg., **59**, *3*, pp. 228–236 (2014).
(27) L. Pierrat, E. Dejaeger, M.S. Garrido, *Models unification for the saturated synchronous machines*, Proc. Int. Conf. on Evolution and Modern Aspects of Synchronous Machines, Zürich, Switzerland, pp. 44–48 (1991).
(28) A.N. El-Serafi, J. Wu, *Saturation representation in synchronous machine models*, Elec. Machines and Power Systems, **20**, pp. 355–369 (1992).
(29) S. Yamamoto, T. Ara, K. Matsuse, *A method to calculate transient characteristics of synchronous reluctance motor considering iron loss and cross-magnetic saturation*, IEEE Trans. Ind. Appl., **43**, *1*, pp. 47–56 (2007).